Reliable determination of chemical state in x-ray photoelectron spectroscopy based on sample-work-function referencing to adventitious carbon: Resolving the myth of apparent constant binding energy of the C 1s peak

Grzegorz Greczynski and Lars Hultman

Greczynski, G., Hultman, L., (2018), Reliable determination of chemical state in x-ray photoelectron spectroscopy based on sample-work-function referencing to adventitious carbon: Resolving the myth of apparent constant binding energy of the C 1s peak, *Applied Surface Science*, 451, 99-103.
https://doi.org/10.1016/j.apsusc.2018.04.226

Reliable determination of chemical state in x-ray photoelectron spectroscopy based on sample-work-function referencing to adventitious carbon: Resolving the myth of apparent constant binding energy of the C 1s peak

G. Greczynski* and L. Hultman

Thin Film Physics Division, Department of Physics (IFM), Linköping University, SE-581 83 Linköping, Sweden

Abstract

The accuracy of chemical-state determination by *x*-ray photoelectron spectroscopy used in contemporary advanced materials research relies on a trustworthy binding energy (BE) referencing method. The C 1s peak corresponding to C-C/C-H bonds of adventitious carbon (AdC), present on a majority of air-exposed samples, is most commonly employed for this purpose, irrespective of whether samples are electrically conducting or not. Contrary to conventional practice, which takes the BE of C 1s peak of AdC as a constant, we find that the C 1s peak position E_B^F varies over an alarmingly large range, from 284.08 to 286.74 eV, depending on the substrate, for nearly a hundred predominantly thin-film samples comprising metals, nitrides, carbides, borides, oxides, and oxynitrides. Our consistent measurements also show that, independent of materials system, E_B^F of the C 1s peak is closely correlated to the sample work function ϕ_{SA}, such that the sum $E_B^F + \phi_{SA}$ is constant, indicating that the electronic levels of the AdC layer align to the vacuum level, rather than to the Fermi level as commonly assumed. This phenomenon can be understood given that the AdC layer is not an inherent part of the analyzed sample and that the interaction to the substrate is weak, showing in that a common Fermi level is not established at the interface. Thus, a straightforward complementary measurement of ϕ_{SA} enables using the C 1s peak of AdC for the purpose of BE-scale calibration for samples exhibiting decent electrical conductivity. This new practice resolves problems

associated with the conventional method and allows for more reliable bonding assignments. It is thus advisable that both ASTM and ISO XPS referencing guides relying on the use of AdC should be reviewed.

* Corresponding author: grzgr@ifm.liu.se; (+46 13 281213)

Keywords: XPS; surface chemistry; adventitious carbon; binding energy reference, work function

Correct measurement of binding energy (BE) values is essential for ~~the~~ unambiguous bonding assignment in x-ray photoelectron spectroscopy (XPS),[1,2] which, since the discovery of the chemical shift in the late 50's,[3,4,5,6] has become the primary analytical tool for assessing surface chemistry in materials science. Reliable XPS analyses require that the BE scale is calibrated, which allows for assessment of the surface chemistry by comparing the recorded BE's of main core-level peaks to the selected standard~~s~~. This is a relatively simple task only for samples that possess an internal BE reference, such as metals, in which case the Fermi edge cut-off that should naturally occur at 0 eV serves this purpose.[7] For the vast majority of specimens though, the problem is not easily resolved which is best proven by the large spread of reported BE values for the atoms present in the same chemical state.[8] This situation is unacceptable as it often leads to an arbitrary spectral interpretation and contradictory results.

In the XPS literature by far the most common procedure for BE scale calibration, irrespective of whether samples are electrically conducting or not, is to use the C 1s signal from the adventitious carbon (AdC) accumulated on the vast majority of surfaces upon exposure to ambient conditions,[1,9] and consisting predominantly of polymeric hydrocarbon species (C-C/C-H), together with a minor component due to carbooxides containing C-O-C and O-C=O bonds.[10] The XPS BE scale is then calibrated by setting the C-C/C-H peak of AdC, quite arbitrarily, at any value in the range 284.0-285.6 eV.[11,12] This inconsistency contradicts the notion of a BE reference, originally intended to be represented by one single value of 285.0 eV, and adds to the large spread of reported BE values for the same chemical species. The extent and popularity of this method contrasts with the documented examples of associated problems reported over the years where C 1s referencing leads to inconsistent results.[13,14,15,16,17,18,19,20]

Recently we demonstrated for a series of transition-metal nitride thin films with a well-defined Fermi edge cut-off serving as an internal BE reference, that the BE of the C 1s peak of adventitious carbon referenced to the Fermi edge E_B^F depends on the work function ϕ_{SA}, and

may vary by as much as 1.44 eV.[21] Such a large substrate influence clearly excludes C 1s peak as a useful energy reference.

Here, we verify our findings on a carefully selected set of nearly one hundred predominantly thin-film samples spanning a wide range of material systems representing metals, nitrides, carbides, borides, oxides, and oxynitrides. We find E_B^F of C 1s peak varying in a disturbingly large range, from 284.08 to 286.74 eV, depending on the substrate. Importantly, independent of the materials system, E_B^F of C 1s peak closely correlates to the sample work function ϕ_{SA}, such that the sum $E_B^F + \phi_{SA}$ is constant at 289.58±0.14 eV. These results confirm that, independent of the materials system and the air exposure time, electronic levels of the AdC layer align to the vacuum level rather than to the Fermi level as commonly assumed, with alarming consequences for BE referencing based on the C 1s peak.

The adventitious carbon layers that are the main focus of this study are accumulated on the surfaces of samples predominantly in the form of thin films grown by magnetron sputtering methods. The materials systems, including metals, transition-metal nitrides, carbides, borides, oxides, and oxynitrides, are listed in the supplementary Table 1. With the aim to maximize sample diversity, all processing parameters are varied over a wide range. The film growth is performed with elemental as well as compound targets, operated either in Ar or in reactive (Ar/N_2) atmosphere. Substrates include Si(001), Al_2O_3(111), and steel. Experiments are performed in various vacuum systems with widely varying background pressures that range from ultra-high vacuum (UHV) to high-vacuum conditions in stationary configuration as well as with substrate rotation typical for industrial coaters. The growth temperature T_s is from RT (23 °C) to 900 °C, while the venting temperature T_v (temperature at which samples are first exposed to the ambient)[22] ranges from RT to 330 °C. Film thicknesses determined from cross-sectional scanning electron microscopy analyses range from 80 to 2560 nm. Samples have been

exposed to the ambient environment for ~~the~~ time periods ranging from several weeks to a few years.

An Axis Ultra DLD XPS instrument from Kratos Analytical with a base pressure better than 1.1×10^{-9} Torr (1.5×10^{-7} Pa) employing monochromatic Al Kα radiation source (hν = 1486.70 eV) is used to acquire core-level XPS spectra from all samples in the as-received state. Work function ϕ_{SA} measurements by ultraviolet photoelectron spectroscopy (UPS) are performed in the same instrument with unmonochromatized He I radiation (hν = 21.22 eV), immediately after XPS analyses. A standard procedure is used in which ϕ_{SA} is assessed from the secondary-electron cutoff energy in the He I UPS spectra by a linear extrapolation of the low-kinetic-energy electron tail towards the BE axis,[23,24] with a precision of ±0.05 eV. ϕ_{SA} obtained from the sputter-cleaned reference Au sample is 5.30 eV, in very good agreement with the textbook values that range from 5.0 to 5.4 eV.[23] The calibration of the binding-energy scale is confirmed by examining sputter-cleaned Au, Ag, and Cu samples according to the recommended ISO standards for monochromatic Al Kα sources that place Au $4f_{7/2}$, Ag $3d_{5/2}$, and Cu $2p_{3/2}$ peaks at 83.96, 368.21, and 932.62 eV, respectively.[25,26] The charge neutralizer was not used in any of the reported experiments.

For all samples that exhibit a non-zero density of states at the Fermi level, in addition to core-level spectra recorded in the as-received state, XPS valence band (VB) spectra are acquired. In all cases the Fermi level cut-off is found to coincide with the 0 eV on the BE scale, which proves that the samples are in a good electrical contact to the spectrometer. The reproducibility of measured E_B^F and ϕ_{SA} values is within ±0.05 eV, as determined by repeating the tests for selected samples.

C 1s core level spectra acquired from all surfaces reveal several chemical states of carbon, as shown for the Ti/Si(001) sample in Figure 1, with a dominant lowest-BE peak due to the aliphatic carbon C-C/C-H, and less intense C-O-C and O-C=O contributions that appear

at higher BE. Figure 2 shows the BE of the C 1s peak corresponding to C-C/C-H bonds of adventitious carbon E_B^F plotted as a function of sample work function ϕ_{SA}. Clearly, and contrary to the common belief which sets the C 1s peak of AdC at 284.5-285.0 eV irrespective of the sample type, E_B^F varies over a wide range, from 284.08 to 286.74 eV, depending on the type of surface adventitious carbon accumulates on. The spread of 2.66 eV is alarmingly large as it reflects the magnitude of the error one makes while aligning XPS spectra to the C 1s peak set at an arbitrarily chosen value lying between 284.5-285.0 eV. It seems that the fact that AdC is not an inherent part of the analyzed sample and as such may not remain in a proper electrical contact by establishing a common Fermi level across the interface, has been overlooked for many years. This result corrupts the spectral interpretation and assignment of the chemical bonds, as the magnitude of chemical shifts is often less than 2.66 eV. The variable C 1s peak position certainly contributes also to the large spread of BE values reported for the same chemical state in XPS data bases.

More importantly, as depicted in Figure 2, E_B^F of the C 1s peak not only varies from sample to sample, but is also closely correlated to the specimen work function ϕ_{SA}. The dashed line representing the linear fit of all data points has a slope of -0.994, which implies that the sum $E_B^F + \phi_{SA}$ is essentially constant. The latter quantity corresponds to the BE referenced to the vacuum level E_B^V.[24,27,28,29] Hence, we can conclude that the binding energy of the C 1s peak of adventitious carbon is fixed with respect to the vacuum level, rather than the Fermi level as commonly assumed. This result can be rationalized by the fact that the adventitious carbon is not an inherent part of the sample. In contrast to specimens where C is either unintentionally or on purpose incorporated into the host material typically resulting in the apparent chemical shift of the C 1s line,[30,31] the bonding between carbon atoms in the AdC layer and the underlying substrate is weak, which makes this case similar to organic films deposited on metals by *ex-situ* techniques such as spin-coating.[32] Such contacts often remain within the Schottky-Mott limit,

where the electronic levels of the adsorbate are determined by the work function of the substrate.[33] As a matter of fact, the process of AdC adsorption is also classified as physical,[10] since the principal species (hydrocarbons) are not chemically reactive and can be readily desorbed by a gentle anneal in vacuum.[34]

To further illustrate the benefits of using E_B^V rather than E_B^F for BE referencing employing the C 1s signal of AdC, all data points are re-plotted in Figure 3 with the same range of vertical scales on both axes (3.5 eV in each case). By referencing to the vacuum level rather than to Fermi level, the standard deviation in the C 1s peak position is reduced by a factor of 4.1. The mean E_B^V value for the C-C/C-H C 1s peak is 289.58±0.14 eV, which is, within the error bars involved, essentially the same as 289.50±0.15 determined in our previous work for the series of transition-metal nitride samples.[21] The standard deviation in this case reflects the combined experimental error of E_B^F and ϕ_{SA} measurement by XPS and UPS, respectively. It is worth ~~to~~ emphasizing that there is no apparent dependence on the air-exposure time, which varies substantially between the examined samples (not shown, see Ref.21). Thus, in order to use the C 1s peak for reliable BE referencing a complementary measurement of ϕ_{SA} is necessary. The best practice is to set the BE of the C 1s peak at 289.58 - ϕ_{SA} eV and to align all other core levels accordingly.

One illustration of practical problems associated with referencing to the C 1s peak of adventitious carbon is shown in Figure 4, where both E_B^F and E_B^V are plotted for a set of $Ti_{1-x}Ta_xN$ samples as a function of the relative Ta content on the cation sublattice, x = Ta/(Ta+Ti). The BE of the C 1s peak of AdC referenced to the Fermi level E_B^F exhibits a linear increase with x from 284.52 eV for x = 0 (TiN) to 285.23 eV with x = 0.93. Figure 5 shows the valence band (VB) spectra as recorded from the same set of $Ti_{1-x}Ta_xN$ samples, with no correction applied to the BE scale. Despite significant variations in the overall shape of the VB spectra with increasing x, the FL cut-off coincides with the 0 eV position on the BE axis,

independent of the Ta content. If one should now follow the widespread practice and apply a BE scale correction by aligning all spectra recorded from $Ti_{1-x}Ta_xN$ films to the C 1s peak of AdC set at 284.5 eV, the FL cut-off would show a gradual shift towards lower BE with increasing *x*, the magnitude of which would correspond to the energy difference between E_B^F plotted in Figure 4 and 284.5 eV. Alarmingly, this re-calibration would result in an unphysical non-zero density of states above the Fermi level for any $x > 0$. In the extreme case of the $x = 0.93$ sample, the FL cut-off would appear at 0.73 eV above the Fermi level. Such mistakes are naturally avoided if the sample work function is measured and E_B^V is used for BE scale calibration. In this particular example, the change in E_B^F with increasing *x* is accompanied by a simultaneous decrease in the sample work function from 4.90 to 4.22 eV, such that the BE referenced to the vacuum level E_B^V is essentially constant at 289.41±0.04 eV (see Figure 4). The latter result agrees with the common-sense notion of ~~a~~ constant energy levels associated with C atoms present in the same chemical environment and provides grounds for more reliable referencing of the XPS spectra.

It should be emphasized, that the spectral referencing by setting the BE of the C 1s peak at 289.58 - ϕ_{SA} eV is not expected to work properly for poorly conducting samples that are prone to charging. This is because the latter phenomenon likely has a different effect on the core level BE's obtained from XPS than on the sample work function determined by UPS, hence, the relationship $E_B^F + \phi_{SA} = 289.58$ eV is not expected to hold. The latter applies irrespectively of whether the measurements are performed with or without the flood gun. There is, however, no apparent reason why the AdC accumulating on non-conducting samples should not exhibit the vacuum level alignment, just as is the case for all specimens included in the present study. Hence, the conventional procedures for charge control, like the XPS referencing guides developed by both ASTM and ISO that explicitly rely on the use of AdC layers,[35,36] need to be modified taking into account our findings.

As a matter of fact, one may think of the relationship $E_B^F + \phi_{SA}$ = 289.58 eV as a criterion to determine the sample charging state, which is not known *a priori*: if $E_B^F + \phi_{SA}$ is significantly larger than 289.58 eV charging likely takes place. This conclusion is made under the assumption, that the sample possesses lateral homogeneity, which is particularly critical if the areas probed by XPS and UPS differ significantly.

In summary, we challenged the commonly used BE referencing method based on the C 1s peak of adventitious carbon for a massive range of metal, nitride, carbide, boride, oxide, and oxynitride thin-film samples that had been exposed to the atmosphere for time periods ranging from several weeks to a few years. We found that the binding energy of the C 1s peak of adventitious carbon corresponding to the C-C/C-H bonds E_B^F varies over an alarmingly large range, from 284.08 to 286.74 eV, depending on the substrate. This 2.66 eV difference, larger than the magnitude of a typical chemical shift, clearly disproves the common assumption of a constant BE of the C 1s peak and leads to the conclusion that the conventional BE referencing method is not reliable. In view of this result, the XPS referencing guides developed by both ASTM and ISO for charge control require thorough revision. We further show that thoughtless application of the standard approach leads to unphysical results such as a density of states above the Fermi level in a series of TiTaN valence-band spectra. Interestingly, independent of the materials system studied and air exposure time, E_B^F of the C 1s peak is closely correlated to the sample work function ϕ_{SA}, such that the sum $E_B^F + \phi_{SA}$, corresponding to the binding energy referenced to the vacuum level E_B^V, is essentially constant at 289.58±0.14 eV. The vacuum-level alignment, being a consequence of a weak interaction between the adventitious carbon layer and the underlying sample, implies that a complementary measurement of ϕ_{SA} allows using the C 1s peak for the purpose of binding-energy scale calibration, at least for samples that exhibit decent electrical conductivity. The C 1s BE should then be set at 289.58 - ϕ_{SA} eV, and all other core levels should be aligned accordingly. The condition that AdC is not an inherent part of the

analyzed sample and as such not necessarily remains in ~~a~~ proper electrical contact in the sense of establishing a common Fermi level, has been overlooked in the literature. Differentiation of the material systems included in this study confirms that the concerned AdC issue is not unique to one class of materials and as such should be considered in everyday XPS practice.

The authors most gratefully acknowledge the financial support of the Knut and Alice Wallenberg Foundation Scholar Grant KAW2016.0358, the VINN Excellence Center *Functional Nanoscale Materials* (FunMat-2) Grant 2016-05156, the Åforsk Foundation Grant 16-359, and Carl Tryggers Stiftelse contract CTS 17:166.

Supplementary material

Tab 1. List of all samples included in the study along with measured binding energy values of the C-C/C-H component of the C 1s spectra of adventitious carbon referenced to the Fermi level E_B^F and to the vacuum level E_B^V, as well as the sample work function ϕ_{SA} assessed by UPS. Numbers in the table should facilitate sample identification in the E_B^F vs. ϕ_{SA} plot shown in Figure 2.

Figure captions

Fig. 1 (color online) C 1s XPS spectra of adventitious carbon acquired from a Ti/Si(001) sample exposed to the ambient atmosphere for several weeks.

Fig. 2 (color online) Binding energy of the C 1s peak corresponding to C-C/C-H bonds of adventitious carbon referenced to the Fermi level E_B^F plotted as a function of sample work function ϕ_{SA} assessed by UPS. All samples are in the form of thin films and have been exposed to the ambient conditions for a time period ranging between several weeks and a few years. Numbers should help to identify samples in the supplementary table.

Fig. 3 (color online) Binding energy of the C 1s peak corresponding to C-C/C-H bonds of adventitious carbon referenced to (i) the Fermi level E_B^F (left axis), and (ii) the vacuum level E_B^V (right axis). To facilitate direct comparison the range of vertical axes is kept constant. Arrows indicate the overall trend observed for E_B^V values to accumulate at 289.58±0.14 eV.

Fig. 4 (color online) Binding energy of the C 1s peak corresponding to C-C/C-H bonds of adventitious carbon accumulated on the surfaces of $Ti_{1-x}Ta_xN$ thin film samples referenced to (i) the Fermi level E_B^F (left axis), and (ii) the vacuum level E_B^V (right axis) and plotted as a function of the Ta content on the cation lattice *x*. To facilitate direct comparison the range of vertical axes is kept constant.

Fig. 5 (color online) Valence-band spectra recorded from the set of $Ti_{1-x}Ta_xN$ thin film samples with varying Ta content on the cation lattice *x*. Data are presented as measured, i.e., no correction of the BE scale has been applied.

References

[1] A. Fahlman, K. Hamrin, J. Hedman, R. Nordberg, C. Nordling, K. Siegbahn, Nature 1966, 210, 4
[2] K. Siegbahn, C. Nordling, A. Fahlman, R. Nordberg, K. Hamrin, J. Hedman, G. Johansson, T. Bergmark, S.-E. Karlsson, I.. Lindgren, and B. Lindberg, "ESCA – Atomic, Molecule and Solid State Structure Studied by Means of Electron Spectroscopy", Almqvist & Wiksells Boktryckeri, Uppsala, Sweden, 1967
[3] E. Sokolowski, C. Nordling, and K. Siegbahn, Phys. Rev. 1958, 110, 776
[4] S. Hagström, C. Nordling, and K. Siegbahn, Z. Phys. 1964, 178, 439
[5] G. Axelson, U. Ericson, A. Fahlman, K. Hamrin, J. Hedman, R. Nordberg, C. Nordling, K. Siegbahn, Nature 1967, 213, 70
[6] R. Nordberg, R.G. Albridge, T. Bergmark, U. Ericson, A. Fahlman, K. Hamrin, J. Hedman, G. Johansson, C. Nordling, K. Siegbahn, B. Lindberg, Nature 1967, 214, 481
[7] J.B. Metson, Surf. Interf. Anal. 1999, 27, 1069
[8] NIST X-ray Photoelectron Spectroscopy Database, Version 4.1 (National Institute of Standards and Technology, Gaithersburg, 2012); http://srdata.nist.gov/xps/. Accessed: 2018-01-16
[9] G. Johansson, J. Hedman, A. Berndtsson, M. Klasson, and R. Nilsson, J. Electron Spectrosc. Relat. Phenom. 1973, 2, 295
[10] T.L. Barr, S. Seal, J. Vac. Sci. Technol. A 1995, 13, 1239
[11] S-H. Lee, E. Yamasue, K. N. Ishihara, H. Okumura, *Applied Catalysis B: Environmental* 93 (2010) 217
[12] B. Psiuk, J. Szade, K. Szot, Vacuum 131 (2016) 14
[13] P. Swift, Surf. Interf. Anal. 1982, 4, 47
[14] S. Kohiki, K. Oki, J. Electron Spectrosc. Relat. Phenom. 1984, 33, 375
[15] S. Kinoshita, T. Ohta, H. Kuroda, Bull. Chem. Soc. Jpn. 1976, 49, 1149
[16] C.R. Werrett, A.K. Bhattacharya, D.R. Pyke, Appl. Surf. Sci. 1996, 103, 403
[17] Th. Gross, M. Ramm, H. Sonntag, W. Unger, H.M. Weijers, E.H. Adem, Surf. Interf. Anal. 1992, 18, 59
[18] A. Pelisson-Schecker, H.J. Hug, and J. Patscheider, Surf. Interf. Anal. 2012, 44, 29
[19] M. Jacquemin, M.J. Genet, E.M. Gaigneaux, and D.P. Debecker, ChemPhysChem 2013, 14, 3618
[20] W. E. S. Unger, Th. Gross, O. Böse, A. Lippitz, Th. Fritz, and U. Gelius, Surf. Interface Anal. 29 (2000) 535
[21] G. Greczynski and L. Hultman, ChemPhysChem 2017, 18, 1507
[22] G. Greczynski, S. Mráz, L. Hultman, J.M. Schneider, Appl. Phys. Lett. 2016, 108, 041603
[23] see for example: Chapter 1 in S. Hűfner "Photoelectron Spectroscopy: Principles and Applications", 3rd Ed. Springer 2003, ISSN 1439-2674
[24] H. Ishii, E. Sugiyama, E. Ito, and K. Seki, Adv. Mat. 1999, 11, 605
[25] M.P. Seah, Surf. Interf. Anal. 2001, 31, 721
[26] ISO 15472, "Surface chemical analysis- x-ray photoelectron spectrometers - calibration of energy scales" (ISO, Geneva, 2001)
[27] H.D. Hagstrum, Surf. Sci. 1976, 54, 197
[28] R.T. Lewis, M.A. Kelly, J. Electron Spectrosc. Relat. Phenom. 20 (1980) 105
[29] M.J. Edgell, D.R. Baer, J.E. Castle, Appl. Surf. Sci. 26 (1986) 129
[30] G. Greczynski, S. Mráz, L. Hultman, J.M. Schneider, Appl. Surf. Sci. 385 (2016) 356
[31] G. Greczynski, D. Primetzhofer, and L. Hultman, Appl. Surf. Sci. 436 (2018) 102
[32] S. Braun, W.R. Salaneck, and M. Fahlman, Adv. Mat. 2009, 21, 1450
[33] E. H. Rhoderick and R.H. Williams, "Metal-Semiconductor contacts", Clarendon Press, Oxford, 1988
[34] G. Greczynski and L. Hultman, Appl. Phys. Lett. 2016, 109, 211602
[35] ASTM E1523-15, "Standard Guide to Charge Control and Charge Referencing Techniques in X-Ray Photoelectron Spectroscopy", ASTM International, West Conshohocken, PA, 2015, www.astm.org
[36] ISO 19318:2004 "Surface chemical analysis - Reporting of methods used for charge control and charge correction"

#	Sample	E_B^F [eV]	ϕ_{SA} [eV]	E_B^V [eV]
1	Al/Si(001)	286.11	3.43	289.54
2	Si/Si(001)	285.51	4.01	289.52
3	Ti/Si(001)	285.29	4.15	289.44
4	V/Si(001)	284.52	5.10	289.62
5	Cr/Si(001)	284.59	4.79	289.38
6	Y/Si(001)	286.41	3.26	289.67
7	Zr/Si(001)	286.12	3.56	289.68
8	Nb/Si(001)	285.37	4.37	289.74
9	Hf/Si(001)	285.31	4.29	289.60
10	Ta/Si(001)	285.73	3.98	289.71
11	W/Si(001)	285.18	4.56	289.74
12	Au (foil)	284.37	5.17	289.54
13	Ag (foil)	284.82	4.89	289.71
14	$Sc/Al_2O_3(111)$	285.97	3.43	289.40
15	Mn/Si(001)	285.21	4.31	289.52
16	$Mo/Al_2O_3(111)$	284.84	4.70	289.54
17	Ni/Si(001)	285.19	4.18	289.37
18	Cu (foil)	285.21	4.23	289.44
19	Mg/Si(001)	286.00	3.46	289.46
20	Y/Si(001), T_v =29 °C	286.74	2.74	289.48
21	Mg/Si(001), T_v =29 °C	286.42	3.11	289.53
22	Al (foil)	286.23	3.14	289.37
23	Fe (foil)	285.67	3.82	289.49
24	TiN/Si(001)	284.52	4.90	289.42
25	VN/Si(001)	284.15	5.16	289.31
26	CrN/Si(001)	284.60	4.83	289.43
27	ZrN/Si(001)	285.49	4.09	289.58
28	NbN/Si(001)	284.76	4.65	289.41
29	MoN/Si(001)	284.08	5.35	289.43
30	HfN/Si(001)	285.52	4.00	289.52
31	TaN/Si(001)	285.08	4.41	289.49
32	WN/Si(001)	284.22	5.23	289.45
33	TiN/Si(001), T_v =29 °C	284.68	4.70	289.38
34	TiN/Si(001), T_v =330 °C	284.65	4.69	289.34
35	TiN/steel	284.62	4.71	289.33
36	$Ti_{0.84}Ta_{0.16}N/Si(001)$	284.70	4.68	289.38
37	$Ti_{0.62}Ta_{0.38}N/Si(001)$	284.72	4.65	289.37
38	$Ti_{0.39}Ta_{0.61}N/Si(001)$	284.92	4.47	289.39
39	$Ti_{0.21}Ta_{0.79}N/Si(001)$	285.09	4.29	289.38
40	$Ti_{0.14}Ta_{0.86}N/Si(001)$	285.21	4.26	289.47
41	$Ti_{0.07}Ta_{0.93}N/Si(001)$	285.23	4.22	289.45
42	$Zr_{0.93}Al_{0.07}N/Si(001)$	285.46	4.18	289.64
43	$Zr_{0.66}Al_{0.34}N/Si(001)$	285.74	4.08	289.82
44	$Zr_{0.75}Al_{0.25}N/Si(001)$	285.59	4.20	289.79
45	$Zr_{0.37}Al_{0.63}N/Si(001)$	285.82	3.79	289.61
46	ZrN/steel	285.45	4.21	289.66
47	$Zr_{0.73}Al_{0.27}N/Si(001)$	285.42	4.24	289.66

48	$Zr_{0.84}Al_{0.16}N$/Si(001)	285.41	4.21	289.62
49	$Cr_{0.82}Al_{0.18}N$/Si(001)	284.77	4.70	289.47
50	$Cr_{0.71}Al_{0.29}N$/Si(001)	284.75	4.72	289.47
51	$Cr_{0.61}Al_{0.39}N$/Si(001)	284.83	4.63	289.46
52	$Cr_{0.54}Al_{0.46}N$/Si(001)	284.92	4.56	289.48
53	$Cr_{0.45}Al_{0.55}N$/Si(001)	284.99	4.51	289.50
54	$Cr_{0.34}Al_{0.66}N$/Si(001)	285.04	4.45	289.49
55	$Cr_{0.23}Al_{0.77}N$/Si(001)	285.04	4.45	289.49
56	$Cr_{0.15}Al_{0.85}N$/Si(001)	285.14	4.37	289.51
57	$Ti_{0.84}Al_{0.16}N$/Si(001)	284.91	4.64	289.55
58	$Ti_{0.75}Al_{0.25}N$/Si(001)	284.80	4.82	289.62
59	$Ti_{0.65}Al_{0.35}N$/Si(001)	284.93	4.70	289.63
60	$Ti_{0.50}Al_{0.50}N$/Si(001)	285.08	4.69	289.77
61	$Ti_{0.46}Al_{0.54}N$/Si(001)	285.20	4.53	289.73
62	$Ti_{0.41}Al_{0.59}N$/Si(001)	285.04	4.65	289.69
63	$Ti_{0.34}Al_{0.66}N$/Si(001)	285.22	4.61	289.83
64	$Ti_{0.24}Al_{0.76}N$/Si(001)	285.41	4.46	289.87
65	TiC/Si(001)	284.92	4.76	289.68
66	VC/Si(001)	284.67	4.97	289.64
67	CrC/Si(001)	284.86	4.83	289.69
68	NbC/Si(001)	284.98	4.82	289.80
69	MoC/Si(001)	284.83	4.93	289.76
70	$Al_{0.10}Mg_{0.07}B_{0.83}$/Si(001)	286.29	3.34	289.63
71	$Al_{0.07}Mg_{0.08}B_{0.85}$/Si(001)	286.18	3.49	289.67
72	$Al_{0.09}Mg_{0.13}B_{0.78}$/Si(001)	286.18	3.44	289.62
73	$Al_{0.08}Mg_{0.08}B_{0.84}$/Si(001)	286.07	3.53	289.60
74	$Al_{0.07}Mg_{0.03}B_{0.90}$/Si(001)	286.18	3.36	289.54
75	$Al_{0.07}Mg_{0.06}B_{0.87}$/Si(001)	286.34	3.36	289.70
76	$Al_{0.08}Mg_{0.16}B_{0.76}$/Si(001)	286.11	3.50	289.61
77	TiB_2/Si(001)	285.40	4.47	289.97
78	ZrB_2/Si(001)	285.59	4.30	289.89
79	Ta_2O_5/Si(001)	286.10	3.48	289.58
80	TiO_2/Si(001)	285.30	4.22	289.52
81	$V_{0.18}Al_{0.31}O_{0.03}N_{0.48}$/Si(001)	284.90	4.75	289.65
82	$V_{0.16}Al_{0.34}O_{0.03}N_{0.47}$/Si(001)	284.92	4.78	289.70
83	$V_{0.16}Al_{0.34}O_{0.04}N_{0.46}$/Si(001)	284.88	4.88	289.76
84	$V_{0.17}Al_{0.33}O_{0.07}N_{0.43}$/Si(001)	285.17	4.49	289.66
85	$V_{0.19}Al_{0.33}O_{0.11}N_{0.38}$/Si(001)	285.05	4.63	289.68
86	$V_{0.20}Al_{0.33}O_{0.17}N_{0.30}$/Si(001)	284.80	4.88	289.68
87	$V_{0.22}Al_{0.30}O_{0.25}N_{0.23}$/Si(001)	284.70	4.97	289.67
88	$V_{0.24}Al_{0.28}O_{0.30}N_{0.18}$/Si(001)	284.67	5.05	289.72
89	$V_{0.19}Al_{0.35}O_{0.38}N_{0.08}$/Si(001)	284.61	5.06	289.67

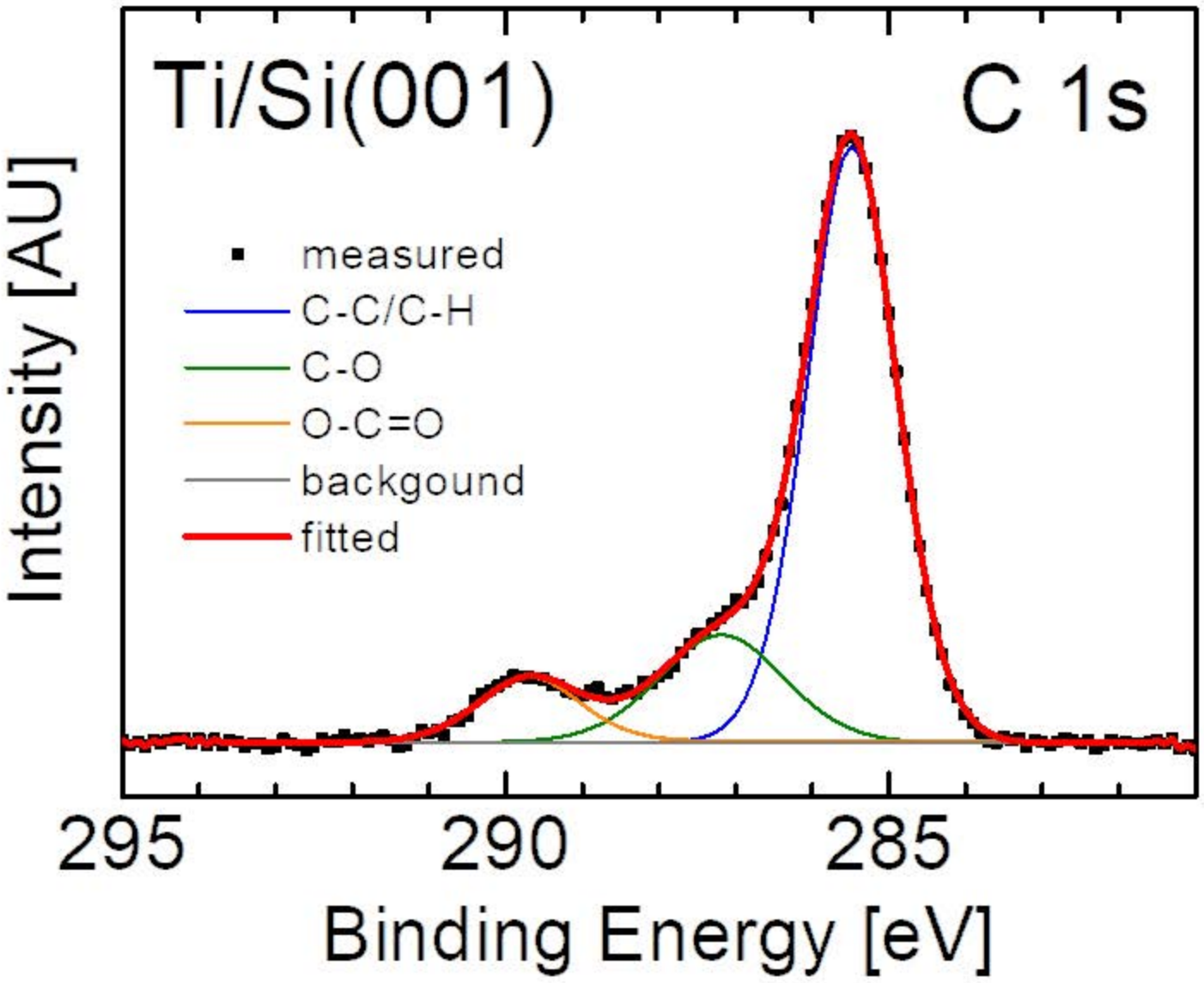
Ti/Si(001)
C 1s
measured
C-C/C-H
C-O
O-C=O
backgound
fitted
Intensity [AU]
295
290
285
Binding Energy [eV]

Fig. 1

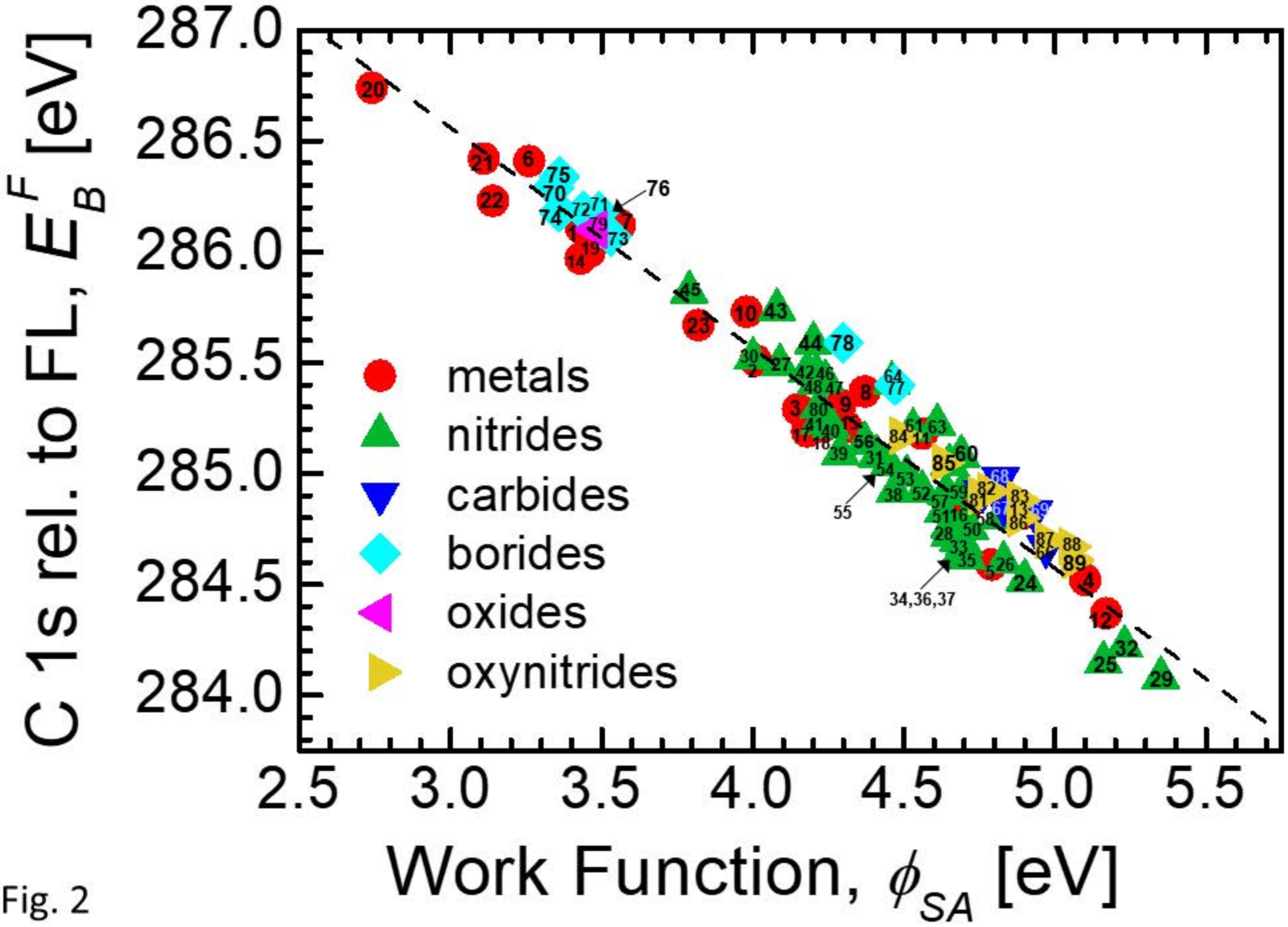
C 1s rel. to FL, E_B^F [eV]
287.0
286.5
286.0
285.5
285.0
284.5
284.0
2.5
3.0
3.5
4.0
4.5
5.0
5.5
Work Function, ϕ_{SA} [eV]
metals
nitrides
carbides
borides
oxides
oxynitrides
55
34,36,37
76

Fig. 2

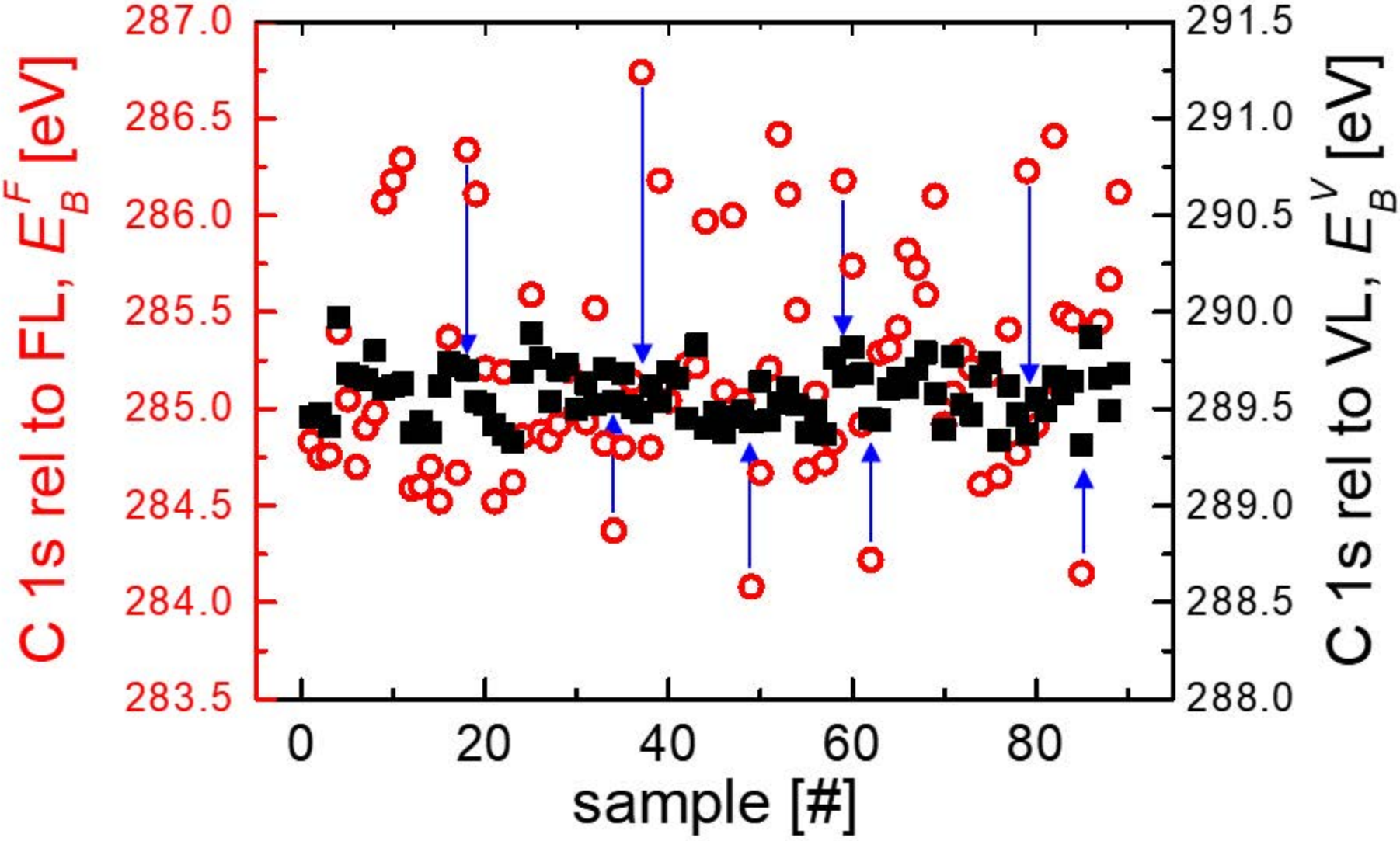
C 1s rel to FL, E_B^F [eV]
C 1s rel to VL, E_B^V [eV]
sample [#]
287.0
286.5
286.0
285.5
285.0
284.5
284.0
283.5
291.5
291.0
290.5
290.0
289.5
289.0
288.5
288.0
0
20
40
60
80

Fig. 3

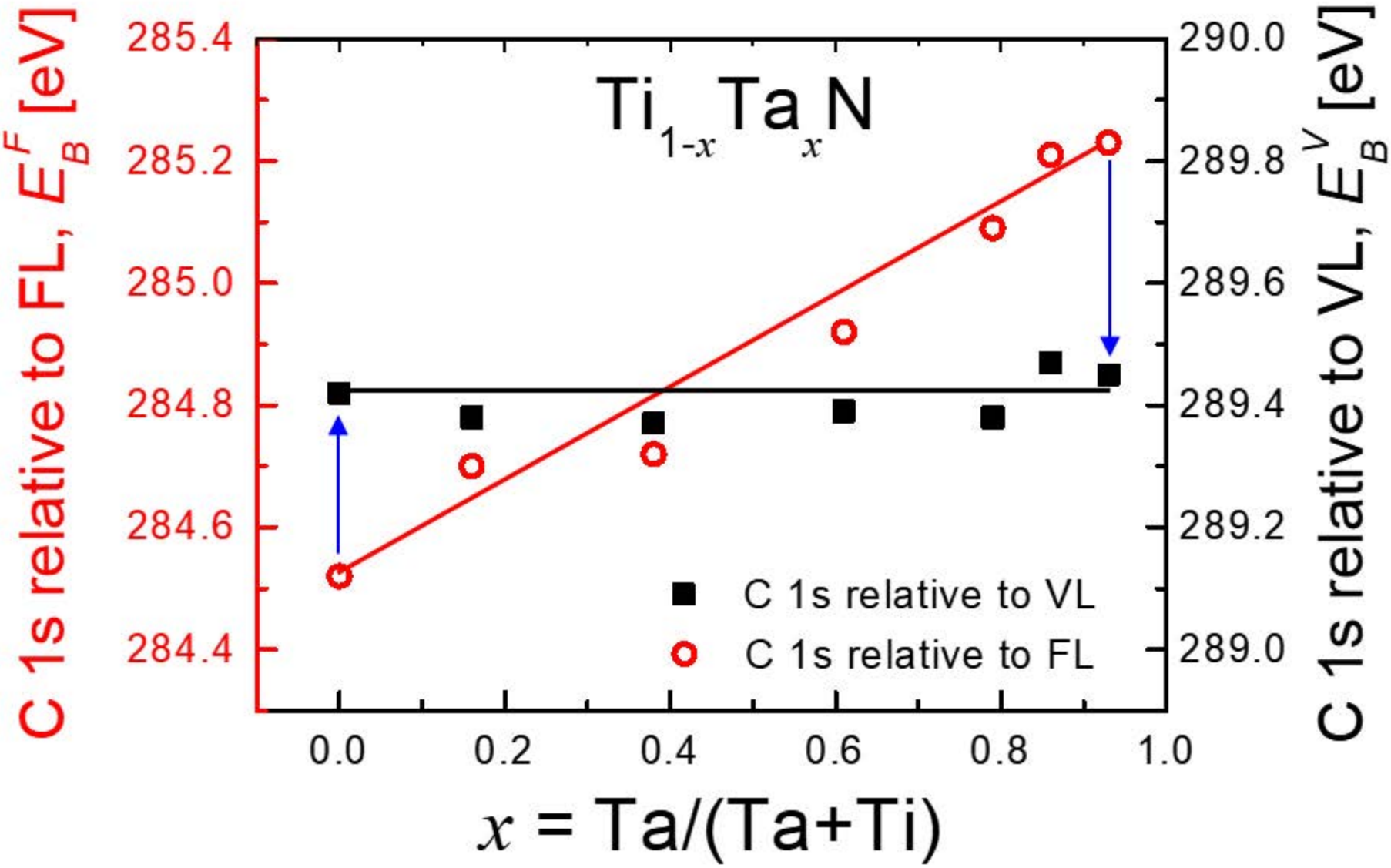
Ti1-xTaxN
C 1s relative to FL, E_B^F [eV]
C 1s relative to VL, E_B^V [eV]
285.4
285.2
285.0
284.8
284.6
284.4
290.0
289.8
289.6
289.4
289.2
289.0
C 1s relative to VL
C 1s relative to FL
0.0
0.2
0.4
0.6
0.8
1.0
x = Ta/(Ta+Ti)

Fig. 4

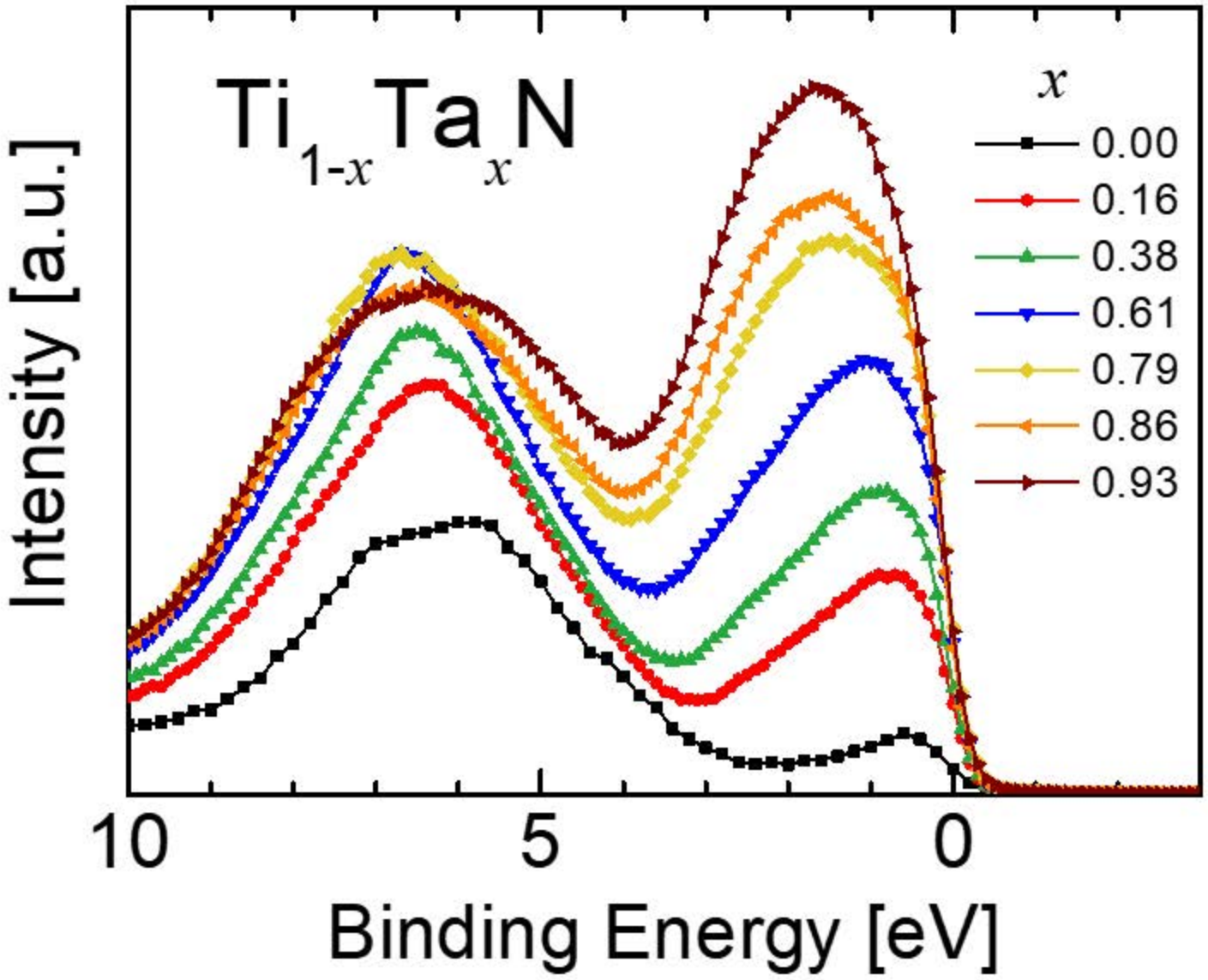
Ti1-xTaxN
x
0.00
0.16
0.38
0.61
0.79
0.86
0.93
Intensity [a.u.]
10
5
0
Binding Energy [eV]

Fig. 5